The Pharma Innovation Journal 2023; 12(7): 2313-2324

www.ThePharmaJournal.com

The Pharma Innovation

ISSN (E): 2277-7695
ISSN (P): 2349-8242
NAAS Rating: 5.23
TPI 2023; 12(7): 2313-2324

www.thepharmajournal.com
Received: 23-06-2023
Accepted: 26-07-2023

**Gangadhar Namwade**
Department of Soil and Water Conservation Engineering, College of Agricultural Engineering and Technology, Anand Agricultural University, Godhra, Gujarat, India

**MM Trivedi**
Polytechnic in Agricultural Engineering, Anand Agricultural University, Dahod, Gujarat, India

**Mukesh Kumar Tiwari**
Department of Soil and Water Conservation Engineering, College of Agricultural Engineering and Technology, Anand Agricultural University, Godhra, Gujarat, India

**GR Patel**
Department of Agricultural Engineering, College of Agriculture, Anand Agricultural University, Vaso, Gujarat, India.

**Bhukya Srinivas**
Department of Soil and Water Conservation Engineering, College of Agricultural Engineering and Technology, Anand Agricultural University, Godhra, Gujarat, India

**Corresponding Author:**
**Gangadhar Namwade**
Department of Soil and Water Conservation Engineering, College of Agricultural Engineering and Technology, Anand Agricultural University, Godhra, Gujarat, India

# Analysis of significant morphometric parameters and sub-watershed prioritization using PCA and PCA-WSM for soil conservation

**Gangadhar Namwade, MM Trivedi, Mukesh Kumar Tiwari, GR Patel and Bhukya Srinivas**

**Abstract**
Knowledge of watershed geometry and geomorphic condition is a prerequisite for developing a watershed management plan. use of morphometric analysis has increased significantly in studies dealing with watershed management mainly for the identification of natural drainage systems and prioritization of sub-watersheds. This study employed morphometric analysis and introduced a hybrid model by integrating geo-informatics and multivariate statistical Modeling to identify the most significant erosion-prone morphometric parameters and prioritize the sub-watersheds of the Hathmati River watershed in Sabarkantha district of Gujarat. This study applied two statistical methods, i.e., principal component analysis (PCA) and PCA's weighted sum model (PCA-WSM) based on correlation matrix approach, to prioritise the sub-watersheds. Boundaries of the sub-watersheds and drainage network were determined in geographic information system using digital elevation model. Then, PCA was applied to define the significant morphometric parameters, while the WSA was employed to determine the weights for the significant parameters and calculate the compound values for priority ranking. During prioritization of sub-watersheds using compound factor values, higher priority was assigned to sub watersheds which yielded lowest compound factor and vice-versa. The drainage density varies from 0.41 $km^2/km^{-1}$ to 1.14 $km^2/km^{-1}$, it is observed that the higher density for the sub watershed SW7 and lower for the SW1. the higher drainage density indicates high runoff potential. Sub-watersheds SW6 to SW7 covering an area of 405 $km^2$ were noted to have highest priorities for soil erosion conservation measures; SW2, SW3 and SW4 had medium priorities; and SW1, and SW5 were assessed with lowest priorities. and the results showed that the integration of PCA and WSA was robust enough to define the significant and most effective parameters with their weighted values for the sub-watershed prioritization. It is anticipated that the prioritization of sub-watersheds would be useful to planners, decision makers, and relevant stakeholders for implementation of soil and water conservation interventions for sustainable natural resources management within watershed.

**Keywords:** Geographic information system, morphometric analysis, principal component analysis, weighted sum model, sub-watershed prioritization

## Introduction
Preservation of natural resources, such as land and water, is the ultimate goal of any watershed planning and management activity (Tomer 2014) [51]. Watershed management is becoming more crucial in conservation planning as a result of the depletion of the watershed resources caused by multiple natural and man-made activities. The world's food production systems are also under peril as aquifers continue to dry up and demands for groundwater increase every day. Also, the significant climatic extremes or hazards led to desertification, drought, and land subsidence. Morphometric analysis is the quantitative measurement of the earth's surface, which assist in the comprehension of a variety of concepts, including drainage basins, geomorphology, mass movements, natural hazards, the development of erosion, etc (Mahmood and Gloaguen, 2012) [20]. The morphometric technique, which uses several indices such as linear, areal, and relief morphometry, is one of the ways to comprehend the hydrological status or flood potential in the drainage basin (Diakakis, 2011, Biswas *et al*., 2014) [10, 4]. Studies related to the quantification of drainage basin morphometric parameters are well established in the literature (Horton, 1945; Poyraz *et al*., 2011; Markose *et al*., 2014; Abdoud & Nofal, 2017; Saha *et al*., 2017; Resmi *et al*.,) 2019) [14, 34, 22, 1, 41, 40]. Understanding the various aspects and characteristics of the basin's hydrological system, particularly its rivers, depends heavily on morphometric studies of drainage basins (Dubey *et al*., 2015; Saha *et al*., 2017; Strahler, 1964) [11, 41, 47].

Understanding the processes that shape the earth's surface requires the application of morphometric analyses, which are quantitative and mathematical explanations of earth's physical characteristics (Clarke, 1966; Saha *et al*., 2017) [7, 41]. Therefore, the quantitative analyses of the basin's morphometric variables are important in understanding the morpho dynamics of the basin's resource potentials (Rajasekhar *et al*., 2020; Resmi *et al*., 2019) [38, 40], structural and tectonic disturbances (Pophrae & Balpande, 2014) [33], possibilities of flood hazard evaluation (Resmi *et al*., 2019; Seta *et al*., 2005) [40, 44], Understanding the interactions between the basin's geology, geomorphology, and climate is important for determining erosion intensity and rates (e.g., Gardiner, 1990; Ozdemir & Bird, 2009). (e.g., Magesh *et al*., 2011; Resmi *et al*., 2019; Singh *et al*., 2014) [19, 40, 45]. Quantitative morphometric analysis of a basin requires measurements of the linear, relief/aerial, and gradient of the channel network as well as the evaluation/measurement of drainage density, network diameter, basin area, etc. These measurements are now being made in a GIS environment, which is different from the traditional methods (e.g., Mesa, 2006; Rai *et al*., 2017; Rajasekhar *et al*., 2020; Resmi *et al*.) [25, 37, 38, 40] (Horton, 1945; Strahler, 1952, 1964) [14, 47]. In this study, GIS-based morphometric analyses have been performed and compared with results abtained from the PCA based analysis for sub watershed prioritization

The main objective of the current study is to assess the morphometric characteristics of the Hathmati River watershed in the Sabarmati basin, which is Gujarat state's one of the hottest and wettest (due to the influence of South-West monsoon) regions due to its location in the subtropical climate zone (Dave H.K 2012) [9]. It is one of the major left-bank tributaries of the Sabarmati River. the major source of irrigation water supply to agricultural land which is the predominant land use land cover present in the study area. In this regard, the sub-watershed have quantified and morphometric properties were calculated in terms of linear, relief, and areal morphometry.

## Materials and Methods

### Description of the study area

The Hathmati River watershed (1309.15km$^2$) has been selected for the study and the location map is shown in Fig. 1. It is located between the longitudes of 23° 50'40" and 24° 02'00" North and latitudes of 72° 44'51" and 73° 15'04" East. The Hathmati is one of the major Left bank tributaries of Sabarmati River located in western India. It originates in Gujarat State's southwest foothills of the Rajasthan range and travels in a southwest direction after travelling a course of 122 km before meeting the Sabarmati on its left bank. The Guhai river is a sub-tributary of Hathmati River. The spatial variation in the rainfall is highest for Hathmati basin amongst all sub-basins of Sabarmati basin (Dave 2012) [9]. It lies in Bhiloda (Sabarkantha district) and rises from Gujarat Malwa Hills. It is considered a hot arid/semi-arid region in western India and experiences hot summer from (March to mid-June with three seasons, the monsoon (kharif, between late June to October), the cooler rabi (November to February) which is dry except occasional rain in November and in the coastal region, and the hot summer season. The rainfall occurs almost entirely in monsoon months (June to September), which receives an average annual rainfall of 864 mm. The maximum dry temperature ranges between 42 °C and 45 °C, which is due to tropical monsoon climate (Dave 2012) [9]. The temperature increases from January onwards having maximum values during May and gradually decreases afterwards. The wind direction is predominantly towards the northeast during the months November to March (www.india-wris.nrsc.gov.in).

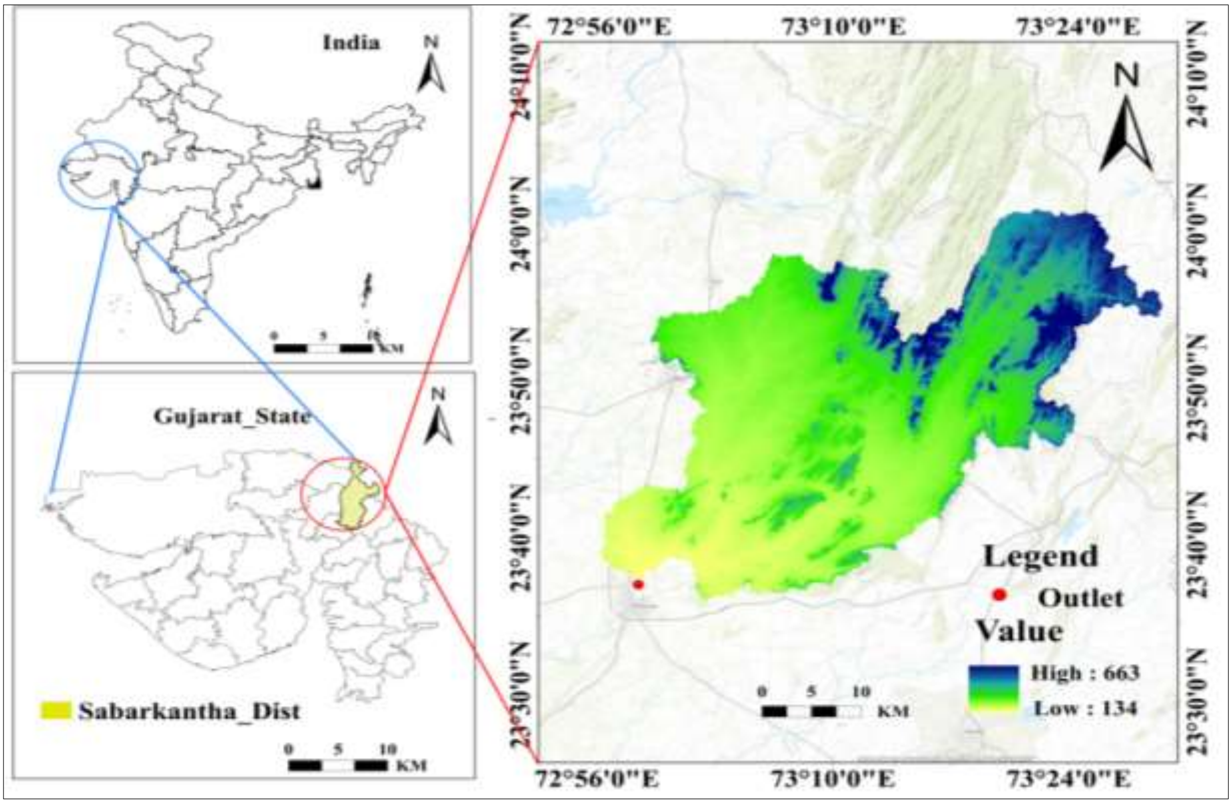


**Fig 1:** Map of the study area

**Data Used**

The sub-watershed boundaries and drainage networks of the study area were identified and extracted using the SRTM-DEM (Fig. 1), which was downloaded in GeoTIFF format with a spatial resolution of 30 m from the USGS Earth Explorer online database. This was done in order to carry out the morphometric study. Singh *et al*. (2014) [45] claims that DEM-based hydrological evaluation at the watershed size is more practical and accurate than other methods currently in use. The following step-by-step process for extraction of stream network and sub watershed delineation, as depicted in Fig. 2, was obtained from the "Arc Hydro Tools Tutorial" manual and used with the Arc Hydro tool in ArcGIS 10.4.1. (ESRI 2009)

**Geomorphometric analysis**

Morphometric studies were conducted to evaluate the overall geometry and features of the Hathmati River SWS. The fundamental parameters, namely, the stream order ($u$), number of streams ($N_u$), stream length ($L_u$), area ($A$), perimeter ($P$), basin length ($L_b$), and total relief ($R_t$) were directly obtained from the drainage map, sub-watershed map, and DEM in the GIS environment, respectively. Later, conventional formulas established by Horton (1932, 1945) [13, 14], Smith (1950) [46], Miller (1953) [27], Schumm (1956) [42, 43], Melton (1957) [23], Nooka Ratnam *et al*. (2005) [28], Strahler (1964) [47] were utilized to determine the linear, areal, shape, and relief features of the examined watershed using these fundamental parameters. In this present study, mean stream length ($L_{sm}$), stream length ratio ($R_L$), bifurcation ratio ($R_b$), RHO coefficient (RHO), length of overland flow ($L_g$) were computed using Eqs. (i), (ii), (iii), (iv), and (v) respectively (Table 1) and clustered into linear parameters. Stream frequency ($F_s$), drainage density ($D_d$), drainage texture ($T$), drainage texture ratio ($D_t$) were computed using Eqs. (vi), (vii), (viii), (ix) respectively (Table 1) and grouped as the areal morphometric parameter. Basin shape ($B_s$), form factor ($F_f$), circularity ratio ($R_c$), elongation ratio ($R_e$), compactness constant ($C_c$) were computed using Eqs. (x), (xi), (xii), (xiii), (xiv), respectively (Table 1) and clustered into shape morphometric parameters. The formula (Eq. i to xiv) are given in Table 1 and the calculated results of the morphometric study are shown in Table 2 (linear MPs), Table 3 (linear MPs), and Table 4 (areal and shape MPs). suggested by Hotelling (1933) [15]. PCA is a widely used data transformation method for streamlining the complexity of multidimensional data. It identifies the variance within a dataset of inter-correlated variables in terms of two or more new pseudo-variables also known as principal components (PCs) (Syms 2019) [48] which were uncorrelated and orthogonal to each other and arranged according to their relative significance. This method can be the best possible approach to simplify the relations among the geo-morphometric features as well as to find the most significant parameters in the sub-watershed scale. Following five simple steps were considered to run the PCA model in the present study (also shown in Fig. 2

**PCA-Based SWS Prioritization**

Pearson (1901) [32] established the principal components, or component analysis, as a statistical method. Hotelling then proposed it (1933) [15]. The complexity of multidimensional data is reduced via the widely used data processing method known as PCA. The variance of an intercorrelated dataset of variables is calculated in terms of two or more additional pseudo-variables, also known as principle components (PCs) (Syms 2019) [48], which were uncorrelated, orthogonal to one another, and organized according to their relative significance. This technique might be the most effective way to locate the most important sub-watershed scale parameters as well as to simplify the relationships between the geomorphometric characteristics. The PCA model depicted in Fig. 2: Following the steps outlined in the IBM-SPSS Statistics guide, all of these mathematical procedures were completed using the software interface of IBM SPSS v26.0 (George and Mallery 2019) [12]. Assigning a preliminary priority rating to the most important EPMPs generated from the Varimax-rotated matrix was the first step in conducting PCA-based SWS prioritization analysis. In this study, the preliminary priority ranks were assigned based on the relative significance of morphometric parameters to soil erosion potential as stated by Nooka Ratnam *et al*. (2005) [28], Aher *et al*. (2014) [2], Prasad and Pani (2017) [35], Malik *et al*. (2019) [21], Pathare and Pathare (2020) [31], and Kumar *et al*. (2021) [17]. These earlier researches proposed that the linear and areal parameters (i.e., $R_b$, $L_g$, $D_d$, $T$, $D_t$, and $F_s$) were directly proportional to runoff and soil erosion potential and were ranked in such a way that the highest value of these morphometric parameters was rated as rank 1, and next highest value was assigned rank 2 and so on. On the other hand, the shape parameters (i.e. $R_c$, $R_e$, $B_s$, and $F_f$) showed an inverse relation with runoff as well as soil erosion potential.

As a result, the preliminary priority rank of this group of parameters was assigned in such a way that parameters with the lowest value received the first rank, and the rest of the ordering followed suit. Finally, the PCA-based compound factors (CF) of each SWS were calculated using Eq. (xv). The SWS that achieved the minimum CF value was received the highest priority and the maximum value received the least priority. And compound factor (CF) assessment can be expressed by Eq. (xvi) (modified after Aher *et al*. 2014; Malik *et al*. 2019) [2, 21]

$$\mathrm{CF} = \frac{\text{sum of all the preliminary ranks of most significant EPMPs suggested by PCA}}{\text{The total number of most significant EPMPs suggested by PCA}} \quad \text{(i)}$$

$$\mathrm{CF} = \mathrm{PPR_{EPMPs}} \times \mathrm{W_{EPMPs}} \quad \text{(ii)}$$

Here $\mathrm{PPR_{EPMPs}}$ denote the weighted factors of each erosion-prone morphometric parameter (EPMP) obtained from the cross-correlation analysis are used to rank the EPMPs in order of preliminary priority. The Hathmati River SWS's ultimate priority ranking was established based on CF in such a way that the lowest value of the compound factor was given the top priority rank, the next lowest value was given the second priority rank, and so on.

Additionally, the SWS were roughly considered into three priority zones, such as high, medium, and low priority zones, depending on their CF values (derived from PCA and PCA-WSM). The outcomes of the above two procedures were compared in order to evaluate erosion-prone sites for efficient conservation planning and management techniques. By choosing the common SWS that falls within each priority zone, this produced a final ranking of the SWS.

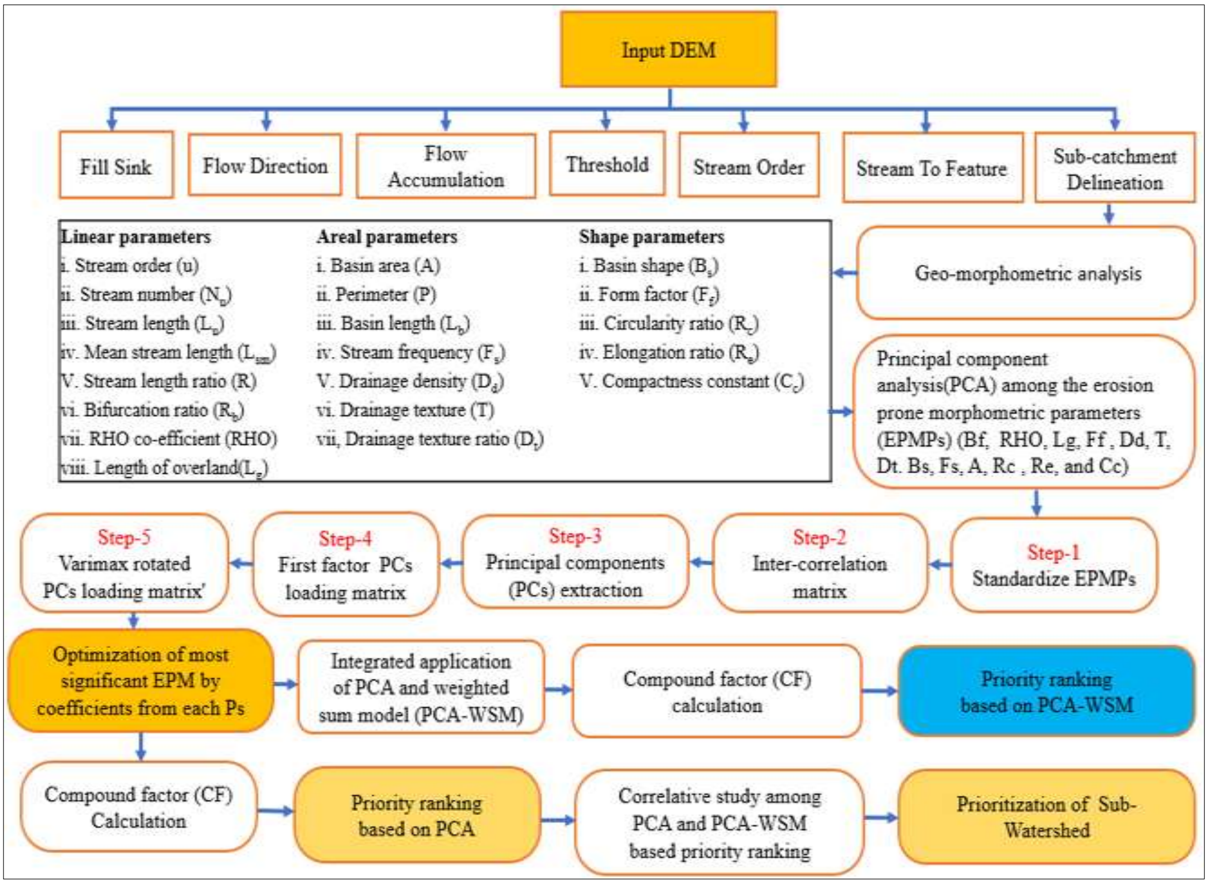


**Fig 2:** Shows a detailed work flow diagram of the current study's approach for extracting drainage lines, defining watersheds, and SWS prioritization

**Table 1:** Formulae were used for computation of morphometric parameters of the Hathmati River sub-watersheds

| Morphologic parameters | Formula | References | Eq. no. |
|---|---|---|---|
| | **Linear parameters** | | |
| Stream order (u) | Hierarchical rank | Strahler (1964) [47] | |
| Stream number ($N_u$) | Total number of stream segments of order 'u' (Calculated from drainage map) | Strahler (1964) [47] | |
| Stream length ($L_u$) | Total length of stream segments of order 'u' (Calculated from drainage map) | Horton (1945) [14] | |
| Mean stream length ($L_{sm}$) | $L_{sm} = L_u/N_u$ | Strahler (1964) [47] | i |
| Stream length ratio ($R_L$) | $R_L=L_u/L_{u-1}$ | Horton (1945) [14] | ii |
| | Where $L_u$=total length of stream segments of order 'u', $L_{u-1}$=total stream length of the previous lower order | | |
| Bifurcation ratio ($R_b$) | $R_b=N_u/N_{u+1}$ | Schumm (1956) [43-43] | iii |
| | Where $N_u$=total number of stream segments of order 'u', $N_{u+1}$=number of segments of the next higher order | | |
| RHO co-efficient (RHO) | $RHO=R_L/R_b$ | Horton (1945) [14] | iv |
| Length of overland flow (Lg) | $L_g=1/2D$ | Horton (1945) [14] | V |
| | **Areal parameters** | | |
| Basin area (A) | The area covered inside the watershed boundaries ($km^2$) (calculated from SWS map) | | |
| Perimeter (P) | The perimeter of SWS (km) (calculated from SWS map) | | |
| Basin length ($L_b$) | Distance between the outlet and farthest point on the basin boundary (km) | Nooka Ratnam *et al*. (2005) [28] | V |
| Stream frequency (Fs) | $Fs=\sum Nu/A$ | Horton (1945) [14] | vi |
| Drainage density ($D_d$) | $Dd=\sum L_u/A$ ($km/km^2$) | Horton (1945) [14] | vii |
| Drainage texture (T) | $T=F_s x D_d$ | Smith (1950) [46] | viii |
| Drainage texture ratio ($D_t$) | $D_t=\sum N_u/P$ | Horton (1945) [14] | ix |
| | **Shape parameters** | | |
| Basin shape (Bs) | $B_s=L^2/A$ | Horton (1945) [14] | x |
| Form factor ($F_f$) | $F_f=A/L_b^2$ ($F_f$<1) | Horton (1932) [13] | xi |
| Circularity ratio ($R_c$) | R,=4xA/$P^2$($R_c$<1) | Miller (1953) [27] | xii |
| Elongation ratio (R) | R,=1.128x$A^{0.5}/L_b$ (Re<1) | Schumm (1956) [42-43] | xiii |
| Compactness constant (C) | $C_c = 0.2821 \times P/A^{0.5}$ ($C_c \geq 1$) | Strahler (1964) [47] | xiv |

## Result and Discussion

### Morphometric Characterization

The study area covers seven sub-watersheds, labeled as SWS-1 to SWS-7 as shown in Fig. 3a. The area of the Hathmati River SWS varies from 113.87 km$^2$ (SWS-7) to 283.75 km$^2$ (SWS-1) (Table 4) with a total area of about 1309.15km$^2$. The morphometric analysis suggests that the Hathmati is 5$^{th}$ order watershed and typically characterized by dendritic drainage patterns.

**Table 2:** SWS wise stream orders and stream lengths of the study area

| SWS No. | Order wise stream numbers (Nu) | | | | | Total (Nu) | Stream lengths (L,,) in km | | | | | Total (Lu) | Mean stream lengths (L.) in km | | | | |
|---|---|---|---|---|---|---|---|---|---|---|---|---|---|---|---|---|---|
| | 1 | 2 | 3 | 4 | 5 | | 1 | 2 | 3 | 4 | 5 | | 1 | 2 | 3 | 4 | 5 |
| SWS-1 | 18 | 5 | 12 | - | - | 35 | 73.8 | 12.3 | 31.4 | | - | 117.5 | 4.1 | 2.5 | 2.6 | - | - |
| SWS-2 | 25 | 16 | 7 | 1 | - | 49 | 66.2 | 51.2 | 9.8 | 0.7 | - | 127.9 | 2.6 | 3.2 | 1.4 | 0.7 | - |
| SWS-3 | 31 | 13 | 13 | 2 | | 59 | 60.7 | 20.8 | 23.7 | 0.7 | - | 105.9 | 2.0 | 1.6 | 1.8 | 0.4 | - |
| SWS-4 | 68 | 36 | 17 | 9 | 4 | 134 | 97.7 | 43.8 | 21.4 | 11.8 | 3.1 | 177.7 | 1.4 | 1.2 | 1.3 | 1.3 | 0.8 |
| SWS-5 | 45 | 22 | 8 | 14 | - | 89 | 68.1 | 26.6 | 12.8 | 13.1 | - | 120.7 | 1.5 | 1.2 | 1.6 | 0.9 | - |
| SWS-6 | 54 | 21 | 27 | 1 | - | 103 | 75.7 | 23.2 | 27.3 | 0.6 | - | 126.8 | 1.4 | 1.1 | 1.0 | 0.6 | - |
| SWS-7 | 85 | 41 | 31 | 3 | - | 160 | 76.8 | 29.8 | 20.5 | 2.9 | - | 130.1 | 0.9 | 0.7 | 0.7 | 1.0 | - |

The study also reveals that the SWS-6 and SWS-7 belong to the 5th order stream and the rest of the sub-watersheds (SWS-3, SWS-2 SWS-1) and belong to the 4th order stream and SWS-5 belongs to 3$^{rd}$ order (Table 2).

**Table 3:** SWS wise linear morphometric parameters of the study area

| SWS No. | Stream length ratio (RL) | | | | | Mean Ri | Bifurcation ratio ($R_b$) | | | | | Mean Br | RHO co-efficient (Rho) | | | | | Mean Rho | Length of overland flow (4) |
|---|---|---|---|---|---|---|---|---|---|---|---|---|---|---|---|---|---|---|---|
| | RL1 | RL2 | RU | RL4 | RL5 | | Rbl | Rb2 | Rb? | Rbs | Rb5 | | 1 | 2 | 3 | 4 | 5 | | |
| SWS-1 | 1.7 | 0.9 | - | - | - | 1.3 | 3.6 | 0.4 | | | - | 2 | 0.5 | 2.3 | 2.6 | - | | 1.4 | 1.2 |
| SWS-2 | 0.8 | 2.3 | 2.1 | | - | 1.7 | 1.6 | 2.3 | 7 | | - | 3.6 | 0.5 | 1 | 0.3 | | | 0.6 | 0.9 |
| SWS-3 | 1.2 | 0.9 | 5 | - | - | 2.4 | 2.4 | 1 | 6.5 | | - | 3.3 | 0.5 | 0.9 | 0.8 | | | 0.7 | 0.9 |
| SWS-4 | 1.2 | 1 | 1 | - | - | 1.2 | 1.9 | 2.1 | 1.9 | - | - | 2 | 0.6 | 0.5 | 0.5 | 0.8 | - | 0.6 | 0.6 |
| SWS-5 | 1.2 | 0.8 | 1.7 | - | - | 1.2 | 2 | 2.8 | 0.6 | - | - | 1.8 | 0.6 | 0.3 | 3 | - | - | 1.3 | 0.6 |
| SWS-6 | 1.3 | 1.1 | 1.7 | | | 1.4 | 2.6 | 0.8 | 27 | | - | 10.1 | 0.5 | 1.4 | 0.1 | - | | 0.7 | 0.6 |
| SWS-7 | 1.2 | 1.1 | 0.7 | - | - | 1 | 2.1 | 1.3 | 10.3 | - | - | 4.6 | 0.6 | 0.8 | 0.1 | - | - | 0.5 | 0.4 |

The mean stream length ratio ($R_L$) varies from 1(SWS-7) to 2.4 (SWS-3), the different SWS (i.e., SWS-1, SWS-2, SWS-3, and SWS-6) shows an increasing trend from lower to higher stream order (Table 3) reflecting the developed geomorphic stage of streams. While other rest of the watershed such as SWS-4, SWS-5, and SWS-7 which indicate the less developed geomorphic stage of streams. The computed mean $R_b$ values range between 3 and 5, except for SWS-6 (10.1) (Table 3), suggesting less intervention of geologic structures to the stream network (Aher *et al*. 2014) [2]. While the higher value of $R_b$ in SWS-6 suggests tectonic control on drainage patterns and excess overland flow. RHO is a significant parameter to assess the storage capacity as well as the physiographic growth of streams (Horton 1945) [14]. The mean RHO coefficient varies from 0.5 (SWS-7) to1.4 (SWS-1) (Table 3). The SWS with lower mean RHO values (SW-7, 6, 2,3, and 4) store less water during floods, and as a result, more erosion takes place at these SWS during high discharge (Rama 2014). The length of the overland flow (Lg) values ranges between 0.4 (SWS-7) and 1.2 (SWS-1) km/km$^2$ (Table 3). Shorter value of Lg in SWS-7 suggest comparatively quick runoff process and high erosion potential than the others (Horton 1945) [14].

**Table 4:** Areal and shape morphometric parameters of the Hathmati River watersheds (SWS)

| SWS NO. | A | P | $L_b$ | $F_s$ | $D_d$ | T | $D_t$ | $B_s$ | $F_f$ | $R_e$ | $R_c$ | $C_c$ |
|---|---|---|---|---|---|---|---|---|---|---|---|---|
| SWS-1 | 283.75 | 108.61 | 32.45 | 0.12 | 0.41 | 0.05 | 0.32 | 3.71 | 0.27 | 0.59 | 0.30 | 1.82 |
| SWS-2 | 234.59 | 85.72 | 29.13 | 0.21 | 0.55 | 0.11 | 0.57 | 3.62 | 0.28 | 0.59 | 0.40 | 1.58 |
| SWS-3 | 180.54 | 89.21 | 25.10 | 0.33 | 0.59 | 0.19 | 0.66 | 3.49 | 0.29 | 0.60 | 0.28 | 1.87 |
| SWS-4 | 204.88 | 91.32 | 26.97 | 0.65 | 0.87 | 0.57 | 1.47 | 3.55 | 0.28 | 0.60 | 0.31 | 1.80 |
| SWS-5 | 133.50 | 84.99 | 21.15 | 0.67 | 0.90 | 0.60 | 1.05 | 3.35 | 0.30 | 0.62 | 0.23 | 2.08 |
| SWS-6 | 158.01 | 85.40 | 23.27 | 0.65 | 0.80 | 0.22 | 1.21 | 3.43 | 0.29 | 0.61 | 0.27 | 1.92 |
| SWS-7 | 113.87 | 66.11 | 19.32 | 1.41 | 1.14 | 1.60 | 2.42 | 3.28 | 0.31 | 0.62 | 0.33 | 1.75 |

Areal parameters such as Fs (Stream frequency), Dd (Drainage density), T (Texture), and Dt (Depth) directly influence surface runoff processes and soil erosion at the scale of surface water systems (SWS) (Melton 1957; Aher *et al*. 2014; Prasad and Pani 2017; Pathare and Pathare 2020) [23, 2, 35, 31]. In the studied SWS, Fs values range from 0.12 to 1.41 (SWS-1 to SWS-7), and Dd values range from 0.41 (SWS-1) to 1.14 (SWS-7) (Table 4). A higher Fs value in SWS-7 indicates excessive runoff and increased erosion during floods (Malik *et al*. 2019) [21]. Moreover, higher Dd and T values in SWS-7 suggest relatively impermeable subsoil conditions and intermediate drainage texture, which promote erosion due to excess runoff depth compared to lower values (Smith 1950) [46].

Shape parameters such as Ff (Form factor), Rc (Circularity ratio), and Re (Elongation ratio) exhibit an inverse relationship with runoff and erosion potentials (Nooka Ratnam *et al*. 2005) [28]. Ff values range from 0.27 (SWS-1) to 0.31 (SWS-7) (Table 4), indicating relatively elongated watersheds with a flatter peak flow over an extended period (Horton 1932) [13]. Rc values range from 0.23 to 0.40 (Table 4), suggesting that the SWS are mostly elongated in shape but less than unity. The lower Rc values in SWS-5 (0.23) and SWS-6 (0.27) indicate higher runoff depth and increased erosion in those regions. The Re values for the Hathmati River SWS are less than unity (0.59–0.62; Table 4), indicating mostly elongated shapes. The lower Re value observed in SWS-1 (0.59) suggests quick surface runoff and higher susceptibility to erosion during floods (Malik *et al*. 2019) [21]. According to Nooka Ratnam *et al*. (2005) [28], Cc (Compactness constant) values are directly proportional to erosion risk assessment factors. Cc values range from 1.58 (SWS-2) to 2.08 (SWS-5) (Table 4). A lower Cc value (<2) in SWS-2 indicates less exposure to erosion risk factors, while higher values (>2) in SWS-5 and SWS-6,1, 7 indicate a higher susceptibility to soil erosion (Aher *et al*. 2014) [2]. Consequently, these SWS require conservation measures.

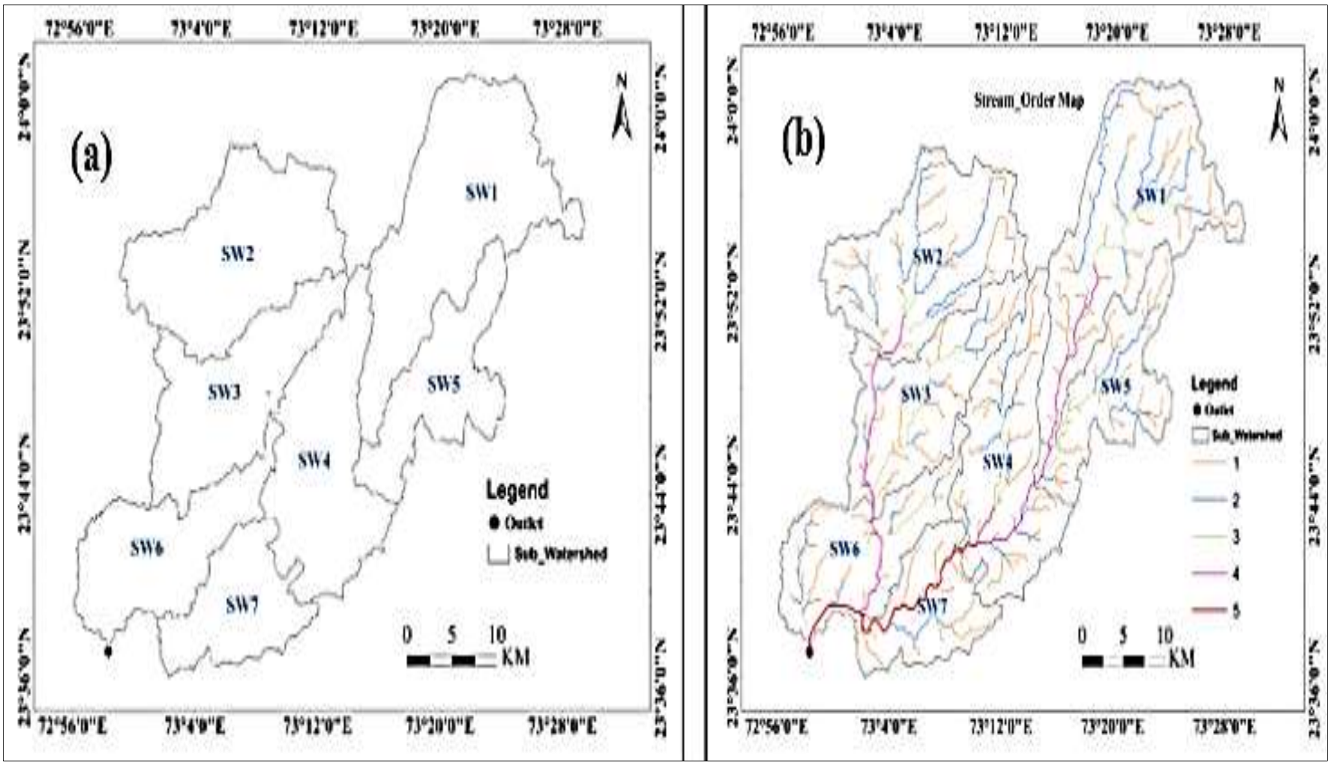


**Fig 3:** (a) shows the Map of sub watersheds and (b) shows the drainage map with 5th order streams

**Inter-correlation of EPMPS.**

The inter-correlation matrix among the 12 selected EPMPs of the Seven SWS as shown in Table 5 typically reveals the degree of relative significances of each constraint among them. In accordance with Meshram and Sharma (2017) [26] and Arefin *et al*. (2020) [3], morphometric parameters demonstrate high significance when the correlation coefficient value is > 0.90, good correlations when the correlation coefficient value is between 0.75 and 0.90, moderate correlation when the correlation coefficient value is between 0.60 and 0.75, and value 0.6 suggests poor correlation among the morphometric parameters. Strong correlations are shown in Table 5 for Fs with T (0.95), Dd (0.96), and Dt (0.98), Dd with T (0.94), T with Dt (0.95), and Bs with Ff and Re (respectively, 0.98 and 0.97). Rc with Cc, Lg with Dd (-0.96) (-0.99). The correlation matrix also reveals the few good correlations between $L_g$ with $B_s$ (0.88), $F_s$ (-0.86), $D_t$ (-0.86), Ff (-0.81), $R_e$ (-0.85) and Fs with Ff (0.85), Re (0.83), Bs (-0.86) and *T with* $F_f$ (0.80), Re (0.73) and $B_s$ (-0.77), $D_t$ with $F_f$ (0.76), $R_e$ (0.74), $B_s$ (-0.78). Most of the parameters in the correlation matrix show poor correlations among them that create difficulties in assembling the parameters into significant components based on their relative importance (Arefin *et al*. 2020) [3]. Consequently, the obtained inter-correlation matrix was considered for PCA to group the EPMPs into principal components PCs that describe the information of the given data.

**Sub watershed prioritization using principal component analysis (PCA)**

In a multivariate data table, PCA, a bilinear analysis technique, offers an understandable summary of the original data. Twelve initial eigenvalues are derived by PCA in the current study and are shown in Table 6. By choosing the components with eigenvalues > 1, the eigenvalue, also known as the Kaiser criteria, is a frequently used indicator for calculating the number of PCs. According to Table 6, the top three components collectively account for 93.56% of the total variance and have eigenvalues > 1. Additionally, Table 6 demonstrates that Component-1's Eigenvalue is 7.41, explaining 61.76% of the total variance, Component-2's Eigenvalue is 2.68, explaining 22.36% of the total variance, and Component 3's Eigenvalue is 1.13, explaining 9.44% of the total variance.

**Table 5:** Inter-correlation matrix of the linear, areal, and shape morphometric parameters of the Hathmati-SWS, which are erosion-prone (calculated in IBM SPSS v.26 software)

| | $B_f$ | *rho* | $L_g$ | $F_s$ | $D_d$ | *T* | $D_t$ | $B_s$ | $F_f$ | $R_c$ | $R_e$ | $C_c$ |
|---|---|---|---|---|---|---|---|---|---|---|---|---|
| $B_f$ | 1.00 | | | | | | | | | | | |
| rho | -0.40 | 1.00 | | | | | | | | | | |
| Lg | -0.27 | 0.47 | 1.00 | | | | | | | | | |
| Fs | 0.24 | -0.43 | -0.86 | 1.00 | | | | | | | | |
| Dd | 0.19 | -0.40 | -0.96 | 0.96 | 1.00 | | | | | | | |
| T | -0.02 | -0.36 | -0.74 | 0.95 | 0.89 | 1.00 | | | | | | |
| Dt | 0.24 | -0.54 | -0.86 | 0.98 | 0.95 | 0.94 | 1.00 | | | | | |
| Bs | -0.30 | 0.28 | 0.88 | -0.86 | -0.89 | -0.77 | -0.78 | 1.00 | | | | |
| Ff | 0.23 | -0.30 | -0.81 | 0.85 | 0.84 | 0.80 | 0.76 | -0.98 | 1.00 | | | |
| Rc | -0.06 | -0.53 | 0.25 | -0.11 | -0.20 | 0.02 | 0.00 | 0.39 | -0.27 | 1.00 | | |
| Re | 0.25 | -0.07 | -0.85 | 0.83 | 0.88 | 0.73 | 0.74 | -0.97 | 0.92 | -0.54 | 1.00 | |
| Cc | 0.04 | 0.55 | -0.29 | 0.12 | 0.24 | 0.00 | 0.01 | -0.43 | 0.32 | -0.99 | 0.58 | 1.00 |

**Table 6:** Total variances explained for the Hathmati-SWS

| Compo. no | Initial Eigenvalues | | | Extraction Sums of Squared Loadings | | | Rotation Sums of Squared Loadings | | |
|---|---|---|---|---|---|---|---|---|---|
| | Total | % of Variance | Cumulative % | Total | % of Variance | Cumulative % | Total | % of Variance | Cumulative % |
| 1 | 7.41 | 61.76 | 61.76 | 7.41 | 61.76 | 61.76 | 7.12 | 59.33 | 59.33 |
| 2 | 2.68 | 22.36 | 84.12 | 2.68 | 22.36 | 84.12 | 2.76 | 22.98 | 82.31 |
| 3 | 1.13 | 9.44 | 93.56 | 1.13 | 9.44 | 93.56 | 1.35 | 11.25 | 93.56 |
| 4 | 0.35 | 2.94 | 96.50 | | | | | | |
| 5 | 0.31 | 2.55 | 99.05 | | | | | | |
| 6 | 0.11 | 0.95 | 100 | | | | | | |
| 7 | 4.51E-16 | 3.76E-15 | 100 | | | | | | |
| 8 | 3.52E-16 | 2.93E-15 | 100 | | | | | | |
| 9 | 1.15E-16 | 9.60E-16 | 100 | | | | | | |
| 10 | 4.82E-17 | 4.01E-16 | 100 | | | | | | |
| 11 | -2.56E-16 | -2.13E-15 | 100 | | | | | | |
| 12 | -6.66E-16 | -5.55E-15 | 100 | | | | | | |

The first-factor loading matrix generated by PCA (Table 7) indicates strong correlations between component-1 and Fs, Dd, Dt, RHO, Bs, Ff, Lg, and Re (>0.9), (0.75-0.90), and moderate correlation with Rc. Component-2 shows strong correlations with Rc and Cc (>0.9) and good correlation with RHO (0.60-0.75), Fs, and T (>0.90), and moderate correlation with Dd. Component-3 exhibits a strong correlation with Bf. However, these results alone do not provide a satisfactory identification of significant components. Hence, the first-factor loading matrix was subjected to rotation using the Varimax algorithm to obtain more reliable correlations.

The analysis reveals that SWS-7 obtains the highest rank (1st) with the lowest CF value of 2.4, while SWS-1 receives the lowest rank (9th) with the highest CF value of 5.4 (Fig. 4a and Table 9). This suggests that SWS-7 is at a high risk for soil erosion and requires an effective soil conservation strategy.

**Table 7:** First factor loading matrix of principal components (PCs) extracted through PCA

| EPMPs | Component | | |
|---|---|---|---|
| | 1 | 2 | 3 |
| Bf | 0.28 | -0.12 | -0.92 |
| rho | -0.38 | 0.78 | 0.31 |
| $L_g$ | -0.94 | 0.02 | 0.07 |
| $F_s$ | 0.96 | -0.17 | 0.10 |
| $D_d$ | 0.98 | -0.07 | 0.09 |
| T | 0.88 | -0.23 | 0.36 |
| $D_t$ | 0.92 | -0.29 | 0.09 |
| $B_s$ | -0.96 | -0.16 | 0.08 |
| $F_f$ | 0.93 | 0.07 | 0.02 |
| $R_c$ | -0.28 | -0.92 | 0.12 |
| $R_e$ | 0.93 | 0.33 | -0.02 |
| $C_c$ | 0.30 | 0.94 | -0.10 |

Table 8 depicts the rotated PC loading matrix, which reveals the largest significant loading was found in PC1 for Lg, Ff, Fs, Dd, T, and Dt (coefficients: 0.90, 0.90, 0.98, 0.98, 0.95, 0.95), in PC2 for Rc and Re (coefficients: -0.96, 0.98), and in PC3 for Bf (coefficient: 0.96). The fact that a high value for a PC loading suggests a strong correlation between the component and the particular morphometric measure should also be kept in mind. Since there are twelve EPMPs, the rotational PC loading matrix obtained by PCA reduces them to the five most crucial EPMPs (Fs, Dd, Cc, Rc, and Bf), which are then taken into account for SWS priority. Using the initial priority ranks of seven SWS as a base, the final priority rankings of those seven SWS and their estimated CF values are given in table 9

**Table 8:** Varimax rotated PCs loading matrix retrieved by PCA orthogonal transformation

| EPMPs | Component | | |
|---|---|---|---|
| | 1 | 2 | 3 |
| $B_f$ | 0.11 | 0.01 | 0.96 |
| rho | -0.41 | 0.69 | -0.46 |
| $L_g$ | -0.90 | -0.11 | -0.24 |
| $F_s$ | 0.98 | -0.04 | 0.10 |
| $D_d$ | 0.98 | 0.05 | 0.09 |
| T | 0.95 | -0.15 | -0.17 |
| $D_t$ | 0.95 | -0.17 | 0.11 |
| $B_s$ | -0.90 | -0.29 | -0.23 |
| $F_f$ | 0.90 | 0.19 | 0.14 |
| $R_c$ | -0.14 | -0.96 | -0.06 |
| $R_e$ | 0.87 | 0.46 | 0.14 |
| $C_c$ | 0.17 | 0.98 | 0.04 |

**Table 9:** PCA-based final prioritization of the Hathmati-SWS

| SWS No. | EPMPs parameters | | | | | Preliminary priority rankings of SWS prioritization based on PCA | | | | | | Final priority |
|---|---|---|---|---|---|---|---|---|---|---|---|---|
| | $B_f$ | $D_d$ | $R_c$ | $C_c$ | $F_s$ | $B_f$ | $F_s$ | $D_d$ | $R_c$ | $C_c$ | CF value | |
| SWS-1 | 2 | 0.41 | 0.3 | 1.82 | 0.12 | 5 | 7 | 7 | 4 | 4 | 5.4 | 7th |
| SWS-2 | 3.6 | 0.55 | 0.4 | 1.58 | 0.21 | 3 | 6 | 6 | 7 | 1 | 4.6 | 6th |
| SWS-3 | 3.3 | 0.59 | 0.28 | 1.87 | 0.33 | 4 | 5 | 5 | 3 | 5 | 4.4 | 5th |
| SWS-4 | 2 | 0.87 | 0.31 | 1.8 | 0.65 | 6 | 3 | 3 | 5 | 3 | 4 | 4th |
| SWS-5 | 1.8 | 0.9 | 0.23 | 2.08 | 0.67 | 7 | 2 | 2 | 1 | 7 | 3.8 | 3rd |
| SWS-6 | 10.1 | 0.8 | 0.27 | 1.92 | 0.65 | 1 | 4 | 4 | 2 | 6 | 3.4 | 2nd |
| SWS-7 | 4.6 | 1.14 | 0.33 | 1.75 | 1.41 | 2 | 1 | 1 | 6 | 2 | 2.4 | 1st |

**Prioritization of sub-watershed using PCA-WSA**

The PCA-WSM is a model that combines PCA and weighted sum analysis to calculate compound factor (CF) values for prioritizing sub watersheds (SWS). It uses significant environmental pollutant parameters (EPMPs) obtained from PCA, including Fs, Dd, Cc, Rc, and Bf. The model constructs a cross-correlation matrix and determines weighting factors for each parameter. The CF values are computed using the preliminary rankings of EPMPs, and the final priority ranking of SWS is determined based on these CF values. SWS-7 receives the highest priority rank (1st), followed by SWS-5, SWS-6, SWS-4, SWS-3, SWS-2, and SWS-1, as indicated by their respective CF values.

**Table 10:** Using cross-correlation analysis, the most significant EPMPs obtained from the PCA model to calculate their final weight-age for SWS prioritization using PCA-adopted weighted sum model (PCA-WSM) (Modified after Aher *et al*. 2014) [2]

| | Most significant EPMPs obtain through PCA model | | | | |
|---|---|---|---|---|---|
| | $B_f$ | $F_s$ | $D_d$ | $R_c$ | $C_c$ |
| Bf | 1.00 | -0.04 | -0.04 | -0.29 | 0.29 |
| Fs | -0.04 | 1.00 | 1.00 | 0.14 | -0.14 |
| Dd | -0.04 | 1.00 | 1.00 | 0.14 | -0.14 |
| Rc | -0.29 | 0.14 | 0.14 | 1.00 | -1.00 |
| Cc | 0.29 | -0.14 | -0.14 | -1.00 | 1.00 |
| Sum of coefficients | 0.93 | 1.96 | 1.96 | 0.00 | 0.00 |
| Final weightages | 0.19 | 0.40 | 0.40 | 0.00 | 0.00 |

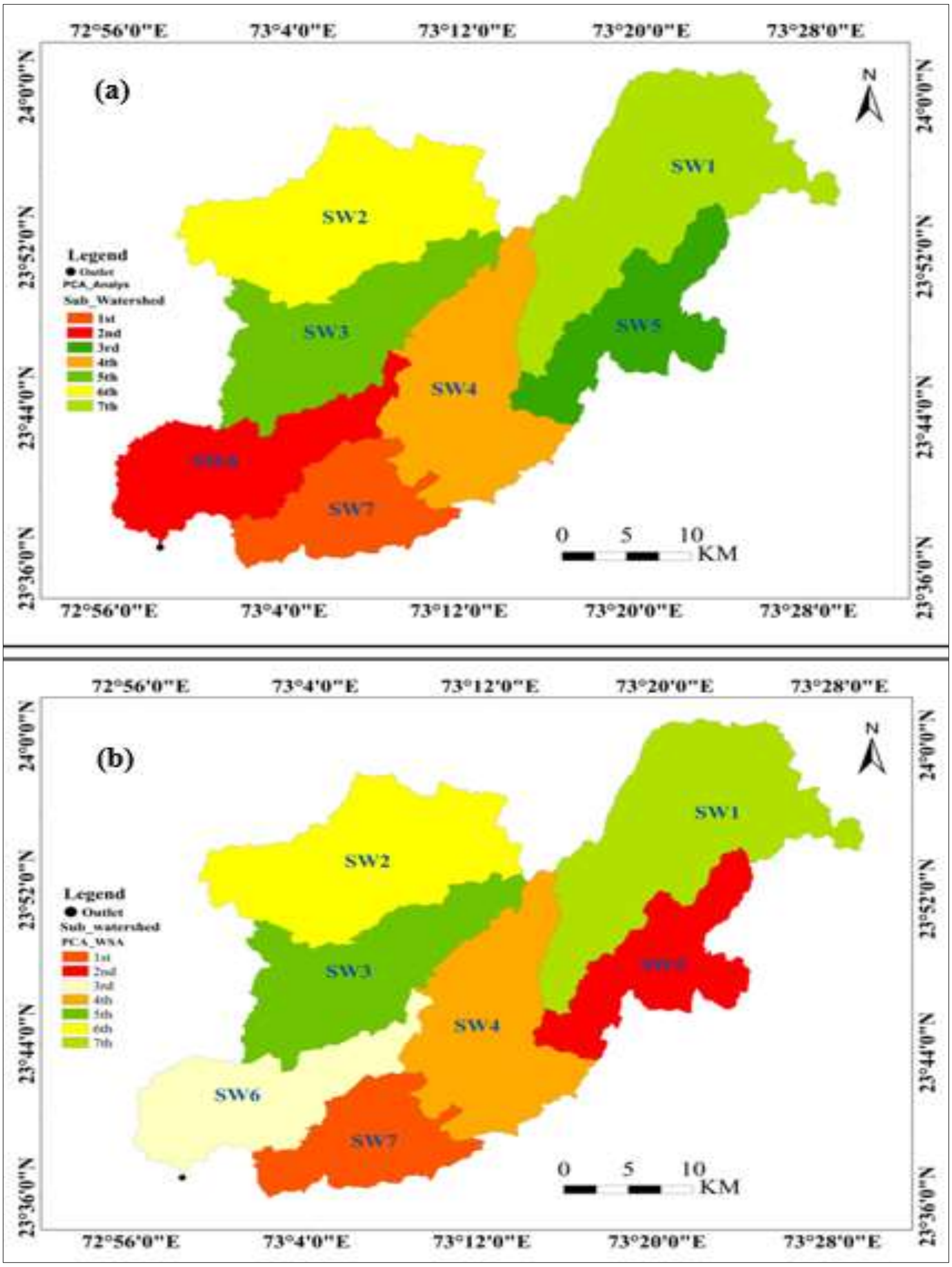


**Fig 4:** SWS prioritization ranking map of the study area based on the compound factor (CF) values derived from (a) the principal component analysis (PCA) method and (b) the PCA adopted weighted sum model (PCA-WSA). Here, the label on the map shows the SWS numbering on both maps

$$CF = (B_f \times 0.19) + (F_s \times 0.40) + (D_d \times 0.40) + (R_c \times 0.00) \times (C_c \times 0.00)$$

**Table 11:** SWS's final priority ranking Based on PCA-WSM compound factor

| | Most significant EPMPs obtain through PCA model | | | | |
|---|---|---|---|---|---|
| | $B_f$ | $F_s$ | $D_d$ | $R_c$ | $C_c$ |
| Bf | 1.00 | -0.04 | -0.04 | -0.29 | 0.29 |
| Fs | -0.04 | 1.00 | 1.00 | 0.14 | -0.14 |
| Dd | -0.04 | 1.00 | 1.00 | 0.14 | -0.14 |
| Rc | -0.29 | 0.14 | 0.14 | 1.00 | -1.00 |
| Cc | 0.29 | -0.14 | -0.14 | -1.00 | 1.00 |
| Sum of coefficients | 0.93 | 1.96 | 1.96 | 0.00 | 0.00 |
| Final weightages | 0.19 | 0.40 | 0.40 | 0.00 | 0.00 |

| SWS no. | SWS prioritization by PCA-WSM | |
|---|---|---|
| | CF value | Final priority |
| SWS-1 | 6.55 | 7th |
| SWS-2 | 5.37 | 6th |
| SWS-3 | 4.76 | 5th |
| SWS-4 | 3.54 | 4th |
| SWS-5 | 2.93 | 2nd |
| SWS-6 | 3.39 | 3rd |
| SWS-7 | 1.18 | 1st |

**Final prioritization of the Hathmati river SWS**

By computing the correlation between the PCA-WSM and PCA-PCA values, the final SWS prioritising was determined. Through this study, the SWS are reclassified into three new priority zones based on the CF values, i.e., CF value of 3.50 signifies the high priority zone, CF value from 3.50 to 5.50 defines the medium priority zone, and CF value > 5.50 denotes the low priority zone (Table 12). The study also demonstrates that the SWS-7, SWS-5, and SWS-6 are classified as high priority zones by the PCA model, whereas the SWS-2, SWS-3, and SWS-4 are classified as medium priority zones and the SWS-1 is classified as low priority zones. SWS-7, SWS-5, SWS-6, and are classified as high priority zones by the PCA-WSM, while SWS-3, SWS-4 and SWS-2 are considered medium priority zones. and the SWS-1 is classified as low priority zones.

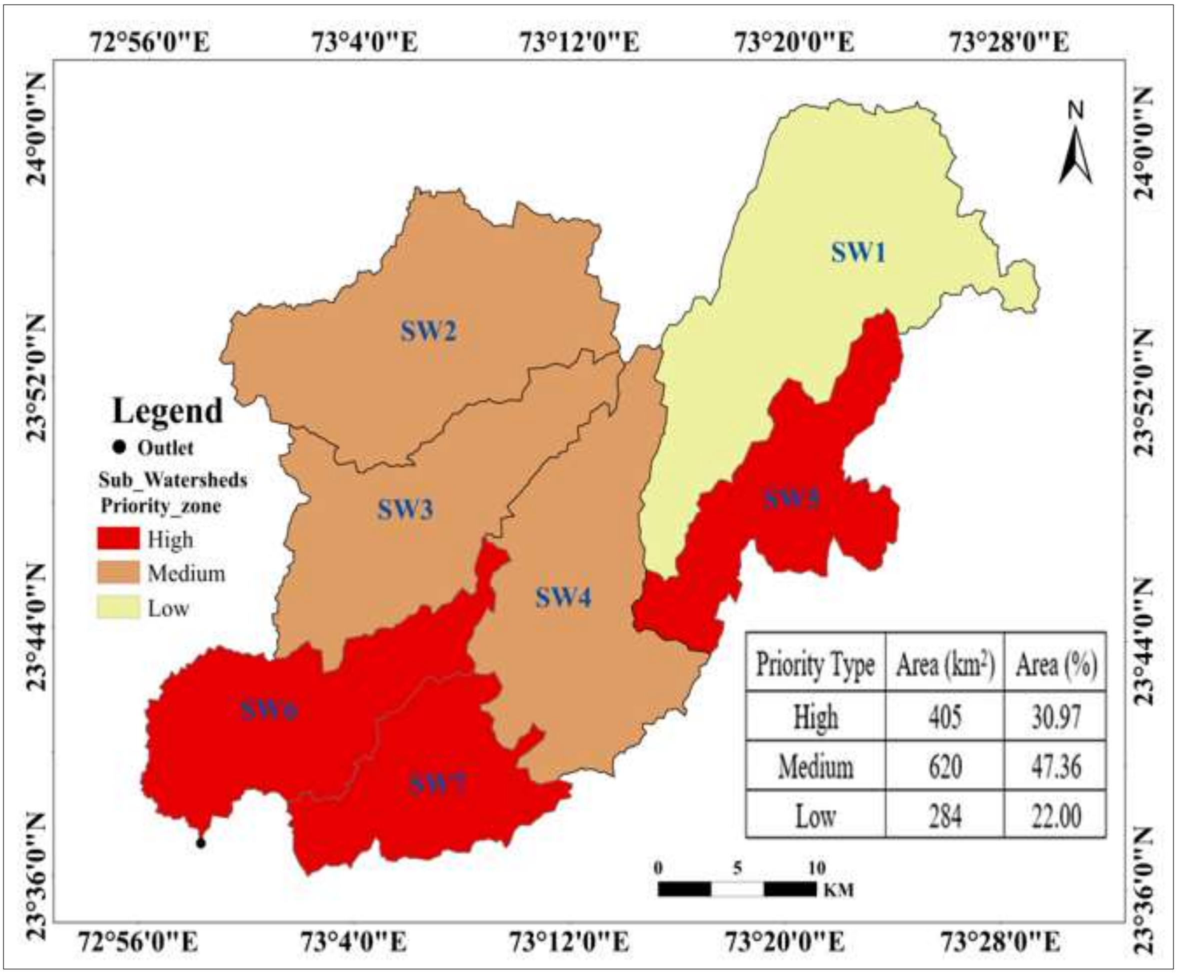


**Fig 5:** Final priority zonation map for Hathmati-SWS based on CF threshold values obtained from the correlation study between PCA and PCA-WSM

**Table 12:** Priority zonation of the Hathmati-SWS based on a comparison of the final ranks obtained from the PCA and the PCA-WSM

| Priority | SWS prioritization by PCA model | | | SWS prioritization by IPCA&WSM model | Common SWS |
|---|---|---|---|---|---|
| | CF value | SWS | | CF value SWS | |
| High | ≤ 3.50 | SWS-7, SWS-5, SWS-6 | | ≤ 4.50 SWS-7, SWS-5, SWS-6, | SWS-7, SWS- 5, SWS-6 |
| Medium | 3.5–5.5 | SWS-2, SWS-3, SWS-4 | 3.5–5.50 | SWS-2, SWS-3, SWS-4 | SWS-2, SWS-3, SWS-4 |
| Low | > 5.0 | SWS-1 | > 5.50 | SWS-1 | SWS-1 |

## Conclusion

Geomorphometric analysis of the Hathmati-SWS was conducted by assessing linear, areal, and shape morphometric parameters to demonstrate their relationship with the watershed hydrology. This work also demonstrates an integrated model for SWS prioritization based on PCA and PCA-WSM that can access the sensitive zone affected by soil erosion. The entire watershed is described as the conventional dendritic drainage system-reflecting 5th order watershed. The stream network map and SWS map computations of twelve EPMPs, namely Bf, RHO, Lg, Fs, Dd, T, Dt, Bs, Ff, Rc, Re, and Cc, were primarily selected as the input variables for PCA. In this work, PCA was carried out using five mathematical processes, including standardisation, inter-correlation analysis, first-factor identification, PCs by extracting eigenvalues > 1, first-factor loading matrix, and rotated matrix calculation. The final output of PCA (rotated matrix) effectively reduces the twelve EPMPs into five most significant EPMPs with the highest axial loading for Fs and Dd (coefficient: 0.98) in PC1, RC and Cc (coefficient: -0.96, 0.98) in PC2, and Bf (coefficient: 0.96) in PC3. The PCA-based prioritising analysis shows that SWS-7, which has the lowest CF values of 2.4, is the high-risk zone for soil erosion, while SWS-1, which has the greatest CF values of 5.4, is the low-risk zone. Additionally, the SWS-7 with the lowest CF value of 1.18 is also in agreement with the results of the PCA-WSM-based watershed prioritisation study, which identifies high-risk SWS in a similar manner. The entire watershed was categorised into three broad categories based on the correlative analysis between these two methodologies, with SWS-5, SWS-6, and SWS-7 being the high-risk zone, SWS-4, SWS-3, SWS-2 being the medium-risk zone, and SWS-1 being the low-risk zone. Results from the combined use of these two techniques (PCA and PCA-WSM) are demonstrated. It is observed that the SWS are located in a high-risk zone (about 30.97% of the entire watershed) should be taken into account for effective and early watershed management planning. Therefore, this research may be viewed as a helpful resource for this study area and river geomorphologists and hydrogeologists to build and implement cutting-edge watershed management plans for vulnerable zones.

## References


1. Abboud IA, Nofal RA. Morphometric analysis of wadi Khumal basin, western coast of Saudi Arabia, using remote sensing and GIS techniques. Journal of African Earth Sciences. 2017;126:58-74.
2. Aher PD, Adinarayana J, Gorantiwar SD. Quantification of morphometric characterization and prioritization for management planning in semi-arid tropics of India: A remote sensing and GIS approach. Journal of Hydrology. 2014;511:850-860. https://doi.org/10.1016/j.jhydrol.2014.02.028
3. Arefin R, Mohir MMI, Alam J. Watershed prioritization for soil and water conservation aspect using GIS and remote sensing: PCA-based approach at northern elevated tract Bangladesh. Appl Water Sci. 2020;10:91. https://doi.org/10.1007/ s13201-020-1176-5
4. Biswas A, Das Majumdar D, Banerjee S. Morphometry governs the dynamics of a drainage basin: analysis and implications. Geography Journal; c2014.
5. Chitsazan M, Rahmani G, Ghafoury H. Investigation of subsidence phenomenon and impact of groundwater level drop on alluvial aquifer, case study: Damaneh-Daran plain in west of Isfahan province, Iran. Modeling Earth Systems and Environment. 2020 Jun;6:1145-61.
6. Chorley RJ, Schumm SA, Sugden DE. Geomorphology, Methuen & Co. Ltd., London; c1984.
7. Clarke JI. Morphometry from maps. Essays in geomorphology. 1966;252:235-74.
8. Dalin C. Sustainability of groundwater used in agricultural production and trade worldwide. In *Global groundwater*. Elsevier; c2021. p. 347-357.
9. Dave HK, *et al*., Study of Rainfall Variation Pattern in Hathmati Basin. ISSN 2250-1991, 2012;1:70-71.
10. Diakakis M. A method for flood hazard mapping based on basin morphometry: application in two catchments in Greece. Natural hazards. 2011;56(3):803-814.
11. Dubey SK, Sharma D, Mundetia N. Morphometric analysis of the Banas River Basin using geographical information system, Rajasthan, India. Hydrology. 2015;3(5):47-57.
12. George D, Mallery P. IBM SPSS statistics 26 step by step: A simple guide and reference. Routledge; c2019.
13. Horton RE. Drainage-basin characteristics. Transactions, American geophysical union. 1932;13(1):350-361.
14. Horton RE. Erosional development of streams and their drainage basins; hydrophysical approach to quantitative morphology. Geological society of America bulletin. 1945;56(3):275-370.
15. Hotelling H. Analysis of a complex of statistical variables into principal components. Journal of educational psychology. 1933 Sep;24(6):417. https://doi. org/10.1037/h0071325
16. Kabir MH, Hossen MN. Impacts of flood and its possible solution in Bangladesh. Disaster Adv. 2019 Oct;12(10):48-57.
17. Kumar V, Sen S, Chauhan P. Geo-morphometric prioritization of Aglar micro watershed in Lesser Himalaya using GIS approach. Model Earth Syst Environ. 2021;7:1269-1279. https://doi.org/10.1007/ s40808-020-01000-8
18. Kumawat A, Meena RS, Rashmi I, Kumar A, Bamboriya SD, Yadav D, Jhariya MK. Crop Residue Management: A Novel Technique for Restoring Soil Health and Sustainable Intensification in India. In Sustainable Intensification for Agroecosystem Services and Management. Springer, Singapore; c2021. p. 229-265.
19. Magesh NS, Chandrasekar N, Soundranayagan JP. Morphometric evaluation of Papanasam and Manimuthar watersheds, parts of Western Ghats, Tirunelveli district, Tamil Nadu, India: A GIS approach. Environmental Earth Science. 2011;642(2):373-381. https:// doi.org/10.1007/s12665-010-0860-4
20. Mahmood SA, Gloaguen R. Appraisal of active tectonics in Hindu Kush: Insights from DEM derived geomorphic indices and drainage analysis. Geoscience Frontiers. 2012 Jul 1;3(4):407-428. https://doi.org/10.1016/j.gsf. 2011.12.002
21. Malik A, Kumar A, Kandpal H. Morphometric analysis and prioritization of sub-watersheds in a hilly watershed using weighted sum approach. Arabian Journal of Geosciences. 2019 Feb;12:1-2. https://doi.org/10.1007/ s12517-019-4310-7
22. Markose VI, Dinesh AC, Jayappa KS. Quantitative

analysis of morphometric parameters of Kali River basin, southern India, using bearing azimuth and drainage (bAd) calculator and GIS. Environmental Earth Science. 2014;72(8):2887-2903. https://doi.org/10.1007/ s12665-014-3193-x
23. Melton MA. An analysis of the relations among elements of climate, surface properties, and geomorphology. Columbia Univ New York; c1957.
24. Merritts D, Vincent KR. Geomorphic response of coastal streams to low, intermediate, and high rates of uplift, Medocino triple junction region, northern California. Geological Society of America Bulletin. 1989 Nov 1;101(11):1373-88.
25. Mesa LM. Morphometric analysis of a subtropical Andean basin (Tucuman, Argentina). Environmental Geology. 2006 Sep;50(8):1235-1242. https://doi. org/10.1007/s00254-006-0297-y
26. Meshram SG, Sharma SK. Prioritization of watershed through morphometric parameters: a PCA-based approach. Appl Water Sci. 2017;7:1505-1519. https://doi.org/10.1007/s13201-015-0332-9
27. Miller VC. A quantitative geomorphic study of drainage basin characteristics in the Clinch Mountain area Virginia and Tennes- see. Columbia Univ, New York; c1953.
28. Nooka Ratnam K, Srivastava YK, Venkateswara Rao V, *et al.* Check dam positioning by prioritization of micro-watersheds using SYI model and morphometric analysis — remote sensing and GIS perspective. J Indian Soc Remote Sens. 2005;33:25-38. https:// doi.org/10.1007/BF02989988
29. Oguchi T. Drainage density and relative relief in humid steep mountains with frequent slope failure. Earth Surface Processes and Landforms: The Journal of the British Geomorphological Group. 1997 Feb;22(2):107-120.
30. Ozdemir H, Bird D. Evaluation of morphometric parameters of drainage networks derived from topographic maps and DEM in point of floods. Environmental Geology. 2009;56(7):1405-1415. https://doi. org/10.1007/s00254-008-1235-y
31. Pathare JA, Pathare AR. Prioritization of micro-watershed based on morphometric analysis and runoff studies in upper Darna basin, Maharashtra, India. Modeling Earth Systems and Environment. 2020;6(2):1123-1130.
32. Pearson K. LIII. On lines and planes of closest fit to systems of points in space. The London, Edinburgh, and Dublin philosophical magazine and journal of science. 1901 Nov 1;2(11):559-572. https://doi.org/10.1080/14786440109462720
33. Pophrae AM, Balpande US. Morphometric analysis of Suketi River basin, Himachal Himalaya, India. Journal of Earth System Science. 2014;123(7):1501-1515. https://doi.org/10.1007/s12040-014-0487-z
34. Poyraz M, Taskın S, Keles K. Morphometric approach to geomorphologic characteristics of Zeytinli Stream basin. Procedia-Social and Behavioral Sciences. 2011;19:322-330.
35. Prasad RN, Pani P. Geo-hydrological analysis and sub watershed prioritization for flash flood risk using weighted sum model and Snyder's synthetic unit hydrograph. Modeling Earth Systems and Environment. 2017 Dec;3:1491-502. https://doi.org/10.1007/s40808-017-0354-4
36. Rahaman KM, Ahmed FRS, Islam N. Modeling on climate induced drought of north-western region, Bangladesh. Modeling Earth Systems and Environment. 2016;2(1):1-21.
37. Rai PK, Mohan K, Mishra S, Ahmad A, Mishra VN. A GIS-based approach in drainage morphometric analysis of Kanhar River Basin, India. Applied Water Science. 2017;7(1):217-232. https://doi.org/10.1007/s13201-014-0238-y
38. Rajasekhar M, Raju GS, Raju RS. Morphometric analysis of the Jilledubanderu river basin, Anantapur District, Andhra Pradesh, India, using geospatial technologies. Groundwater for Sustainable Development. 2020 Oct 1;11:100434. https://doi.org/10.1016/j.gsd. 2020.100434
39. Rama VA. Drainage basin analysis for characterization of 3rd order watersheds using Geographic Information System (GIS) and ASTER data. Journal of Geomatics. 2014 Oct;8(2):200-210.
40. Resmi MR, Babeesh C, Achyuthan H. Quantitative analysis of the drainage and morphometric characteristics of the Palar River basin, Southern Peninsular India; using bAd calculator (bearing azimuth and drainage) and GIS. Geology, ecology, and landscapes, 2019, 3(4).
41. Saha A, Tomar S, Rana A, Singh P. Morphometric and hydrological analysis of Krishni River watershed, Utar Pradesh, India: Using Remote Sensing and GIS Techniques. In 18th ESRI India User Conference; c2017.
42. Schumm SA. Evolution of drainage systems and slopes in badlands at Perth Amboy, New Jersey. Geological society of America bulletin. 1956 May 1;67(5):597-646.
43. Schumm SA. Evolution of drainage systems and slopes in badlands at Perth Amboy, New Jersey. Geological society of America bulletin. 1956 May 1;67(5):597-646.
44. Della Seta MA, Del Monte MA, Pascoli AL. Quantitative geomorphic analysis to evaluate flood hazards. Geografia Fisica e Dinamica Quaternaria. 2005;28(1):117-24.
45. Singh P, Gupta A, Singh M. Hydrological inferences from watershed analysis for water resource management using remote sensing and GIS techniques. The Egyptian Journal of Remote Sensing and Space Science. 2014 Dec 1;17(2):111-21. https://doi.org/10.1016/j.ejrs.2014.09.003
46. Smith KG. Standards for grading texture of erosional topography. American journal of Science. 1950 Sep 1;248(9):655-68.
47. Strahler AN. Quantitative geomorphology of drainage basin and channel networks. Handbook of applied hydrology; c1964.
48. Syms C. Principal components analysis. Encyclopedia of ecol- ogy. Elsevier, Amsterdam; c2019. p. 566-573
49. Thomas J, Joseph S, Thrivikramji KP, Abe G, Kannan N. Morphometrical analysis of two tropical mountain river basins of contrasting environmental settings, the southern Western Ghats, India. Environmental Earth Sciences. 2012;66(8):2353-2366.
50. Tomer MD. Watershed management. Reference module in earth systems and environmental sciences. Elsevier, Amsterda; c2014.